K^+ Channel Inactivation Mediated by the Concerted Action of the Cytoplasmic N- and C-Terminal Domains

Henry H. Jerng and Manuel Covarrubias
Department of Pathology, Anatomy and Cell Biology, Jefferson Medical College, Philadelphia, Pennsylvania 19107 USA

ABSTRACT We have examined the molecular mechanism of rapid inactivation gating in a mouse Shal K^+ channel (mKv4.1). The results showed that inactivation of these channels follows a complex time course that is well approximated by the sum of three exponential terms. Truncation of an amphipathic region at the N-terminus (residues 2–71) abolished the rapid phase of inactivation (τ = 16 ms) and altered voltage-dependent gating. Surprisingly, these effects could be mimicked by deletions affecting the hydrophilic C-terminus. The sum of two exponential terms was sufficient to describe the inactivation of deletion mutants. In fact, the time constants corresponded closely to those of the intermediate and slow phases of inactivation observed with wild-type channels. Further analysis revealed that several basic amino acids at the N-terminus do not influence inactivation, but a positively charged domain at the C-terminus (amino acids 420–550) is necessary to support rapid inactivation. Thus, the amphipathic N-terminus and the hydrophilic C-terminus of mKv4.1 are essential determinants of inactivation gating and may interact with each other to maintain the N-terminal inactivation gate near the inner mouth of the channel. Furthermore, this inactivation gate may not behave like a simple open-channel blocker because channel blockade by internal tetraethylammonium was not associated with slower current decay and an elevated external K^+ concentration retarded recovery from inactivation.

INTRODUCTION

A subclass of neuronal A-type K^+ currents activates in the subthreshold range of membrane potentials and inactivates rapidly when the membrane is depolarized. The time courses of inactivation and recovery from inactivation of these currents are the properties that primarily determine the interspike interval in neurons that display repetitive spike firing (Hille, 1992). K^+ channel subunits encoded by *Shal* genes are believed to be one of the main components underlying the subthreshold A-type K^+ current in neuronal cell bodies (Salkoff et al., 1992; Sheng et al., 1992; Serodio et al., 1994, 1996). However, we do not know the molecular mechanisms that underlie inactivation gating of Shal K^+ channels.

In ShakerB K^+ channels, two distinct mechanisms of inactivation have been recognized (Choi et al., 1991). The first underlies rapid inactivation and is determined by a sequence of about 20 amino acids at the N-terminus of the ShakerB polypeptide (Hoshi et al., 1990; Zagotta et al., 1990). Hydrophobic and basic amino acids within this region are essential in establishing rapid inactivation (Murrell-Lagnado and Aldrich, 1993a,b). A similar conclusion has been reached with two mammalian K^+ channels (Tseng-Crank et al., 1993; Covarrubias et al., 1994). These observations indicated that the N-terminal region of these K^+ channels is the inactivation gate acting as a positively charged tethered particle that occludes the inner mouth of the pore when the channel opens (Demo and Yellen, 1991; Ruppersberg et al., 1991). Although in a tetrameric ShakerB K^+ channel there are four N-terminal inactivation gates, one is sufficient and necessary to cause inactivation (Mackinnon et al., 1993). This mechanism of inactivation is known as N-type. The second type underlies typically slower inactivation and is determined by residues within the putative permeation pathway, mainly in the sixth transmembrane segment S6 and the S5-S6 loop (Hoshi et al., 1991; Lopez-Borneo et al., 1993). This mechanism is known as C-type. Various studies now suggest that C-type inactivation is due to constriction of the outer mouth of the pore, which results from a cooperative conformational change involving all subunits of the channel tetramer (Ogielska et al., 1995; Panyi et al., 1995; Liu et al., 1996). Although C-type inactivation still occurs in the absence of the N-terminal region, it is faster in the presence of N-type inactivation, suggesting that they are partially coupled (Hoshi et al., 1991; Baukrowitz and Yellen, 1995).

By analogy to ShakerB K^+ channels, it has been suggested that Shal K^+ channels may inactivate by N-type and C-type inactivation (Baldwin et al., 1991; Pak et al., 1991). However, evidence of such mechanisms in Shal K^+ channels has remained uncertain. To elucidate the structural basis of inactivation in Shal K^+ channels, we created a series of N-terminal and C-terminal deletions and point mutations that eliminated charged residues within the N- and C-terminal domains of mKv4.1. These mutations did not affect residues within the core of the polypeptide (S1–S6). Wild-type and mutant channels were expressed in *Xenopus* oocytes and studied using whole-oocyte voltage clamp. The results revealed that an amphipathic region at the N-terminus and a largely hydrophilic (and mostly basic) domain at the C-terminus are critical determinants of rapid

Received for publication 30 July 1996 and in final form 4 October 1996.
Address reprint requests to Dr. Manuel Covarrubias, Department of Pathology, Anatomy and Cell Biology, Jefferson Medical College, 1020 Locust St. JAH 245, Philadelphia, PA 19107. Tel.: 215-503-4341; Fax: 215-923-2218; E-mail: covarru1@jeflin.tju.edu.

0006-3495/97/01/163/12 $2.00

inactivation in mKv4.1. By contrast to what is found with ShakerB K^+ channels, our experiments demonstrate that the hydrophilic C-terminus (most likely cytoplasmic) is a novel component of the molecular machinery that controls rapid inactivation gating in mKv4.1 K^+ channels. In addition, experiments with tetraethylammonium (TEA) and an elevated external K^+ concentration revealed that the mechanism of inactivation of these channels may not involve open-channel blockade.

MATERIALS AND METHODS

Molecular biology

mKv4.1 was cloned in pBluescript II KS (Stratagene, La Jolla, CA). Δ2-71 was generated by partially digesting pBluescript with *Eco*RI and *Sac*I, isolating the desired truncated cDNA, and cloning into the *Eco*RI site of a customized vector (pBluestart) with ATG immediately upstream of that site. Δ556-651 was created by digesting pBluescript-mKv4.1 with *Sph*I and *Xba*I blunt-ending with Klenow, and allowing self-ligation to produce an in-frame stop codon. Δ457-651 was generated by digesting with *Xho*I, isolating and blunt ending the truncated cDNA, and cloning it between the blunt-ended *Xho*I and *Xba*I sites of pBluescript, resulting in a 3′ in-frame stop codon. Δ494-651 was generated by the polymerase chain reaction (using a 5′ primer located upstream of the T3 promoter and a 3′ primer that contained the mKv4.1 sequence up to position 494, the in-frame stop codon, and the *Xba*I site). The truncated product was cloned into pBluescript. Δ422-651 was similarly generated by the polymerase chain reaction. Double deletion mutants were also generated by PCR using a 5′ upstream primer containing a *Hin*dIII site and Kozak's sequence, and specific 3′ primers were used to generate Δ494-651 and Δ422-651. Point mutations were created by oligonucleotide-directed mutagenesis using the Altered Sites II in vitro Mutagenesis System (Promega, Madison, WI). All mutations were confirmed by sequencing using a commercial dideoxy method according to manufacturer specifications (Bio-Rad, Hercules, CA), or by automated sequencing (Nucleic Acid Facility, Jefferson Cancer Institute). Capped cRNA for oocyte injection was produced by in vitro transcription using Megascript or Message Machine driven by T3 RNA polymerase (Ambion, Austin, TX). SP6 RNA polymerase was used for site-directed mutants (see above).

Oocyte injection and electrophysiology

Wild-type and mutant mKv4.1 cRNA was microinjected into defolliculated *Xenopus* oocytes (~50 ng/cell) using a Nanoject microinjector (Drummond, Broomall, PA). Whole-oocyte currents were recorded 2–10 days postinjection using the two-microelectrode voltage-clamp technique (TEV-200; Dagan Corp., Minneapolis, MN). Microelectrodes were filled with 3 M KCl (tip resistance was <1 MΩ). Bath solution contained 96 mM NaCl, 5 mM KCl, 1.8 mM $CaCl_2$, 2 mM $MgCl_2$, 10 mM HEPES (pH 7.4, adjusted with NaOH). In some experiments with low-expressing oocytes, we supplemented the bath solution with 100–500 μM diisothiocyanatostilbene-2,2′-sulfonic acid (DIDS) to block endogenous Ca^{2+}-activated Cl^- conductance and phospholemman-like currents (Kowdley et al., 1994). Current traces (generally 900-ms depolarizations) were low-pass filtered at 1 kHz and digitized at 500 μs/point. The average voltage offset recorded at the end of an experiment was generally small (−0.4 ± 2.5 mV, n = 38) and was not subtracted from the command voltage. Correction was applied when offsets appeared to be greater than one standard deviation. The leak current was subtracted off-line, assuming ohmic leak. Capacitive currents were also subtracted off-line, using a scaled noise-free template generated from a current trace with no active time-dependent currents (at −80 mV). Patch-clamp recording of macroscopic currents was conducted as described before (Chabala et al., 1993). Patch pipettes were constructed from Corning glass 7052 (Warner Instrument Corp., Hamden, CT). The pipette solution had the composition of the bath solution described above. The internal solution for inside-out patches contained 98 mM KCl, 0.5 mM $MgCl_2$, 1.0 mM EGTA, 10 mM HEPES (pH 7.2, adjusted with KOH). Passive leak and capacitive transients from macropatch currents were subtracted on-line using a P/4 procedure. TEA was dissolved in internal solution (see above) and applied to the internal side of inside-out patches by moving the patch pipette to the mouth of a glass capillary leaking TEA. Macropatch currents were low-pass filtered at 500 Hz using an 8-pole Bessel filter (Frequency Devices, Haverhill, MA) and digitized at 500 μs/point. Experiments were conducted at room temperature (22–24°C) or at 23°C using a temperature-controlled microscope stage (PDMI-2; Medical Systems Corp., Greenvale, NY).

Data acquisition and analysis

Voltage-clamp protocols and data acquisition were controlled by a 486 desktop computer interfaced to a 12-bit A/D converter (Digidata 1200 using pClamp 6.0; Axon Instruments, Foster City, CA). Data analysis was conducted using Clampfit (pClamp 6.0; Axon Instruments) or Sigmaplot (Jandel, San Rafael, CA). Current decay $I(t)$ was described assuming a sum of exponential terms as shown below:

$$I(t) = A_0\exp(-t/\tau_0) + \cdots + A_n\exp(-t/\tau_n) + A_\infty,$$

where A_0 and A_n are the amplitudes of the exponential terms and τ_0 and τ_n are the corresponding time constants. A_∞ is a constant that represents the steady-state level of the current. No more than three terms were used to describe current decay. To obtain the best fit we used a Simplex algorithm or a Chebyshev transform (according to the pClamp 6.0 user's manual). The two methods gave identical results. The second method, however, converged significantly faster. Multiexponential fits of current relaxations can be sensitive to cursor position. To determine left cursor position and standardize our fitting procedure, the current trace was differentiated. On the original trace, the left cursor was placed at the time that corresponded to the fastest change in the declining phase of the current. The right cursor was placed at the end of the trace. The quality of the fits was evaluated visually by plotting the residuals of the fit (Figs. 1 and 4). Unless indicated otherwise, data are presented as mean ± SD.

RESULTS

mKv4.1 exhibits complex inactivation kinetics in intact *Xenopus* oocytes

mKv4.1 K^+ channels were expressed in *Xenopus* oocytes, and standard two-microelectrode voltage clamp was used to study macroscopic currents. We found that after step depolarizations to positive membrane potentials, the expressed currents rose quickly and decayed following a complex nonexponential time course (Fig. 1, *A* and *B*). At membrane potentials above −10 mV, at least three time constants (slow, intermediate, and fast) were necessary to satisfactorily describe the decay of the current (Fig. 1, *A–D*; compare the residuals of two-exponential fits against those of fits assuming the sum of three-exponential terms). Generally, current decay at −20 and −30 mV was well described by the sum of two exponentials, whereas at −40 mV a single exponential was sufficient (Fig. 1). Time constants and fractional amplitudes of the exponential components were weakly voltage dependent (Fig. 2). The fast time constant (τ_f) exhibited the largest change, decreasing twofold between −10 and +30 mV. Fit parameters were independent of peak current size between 1 and 30 μA. Therefore, the

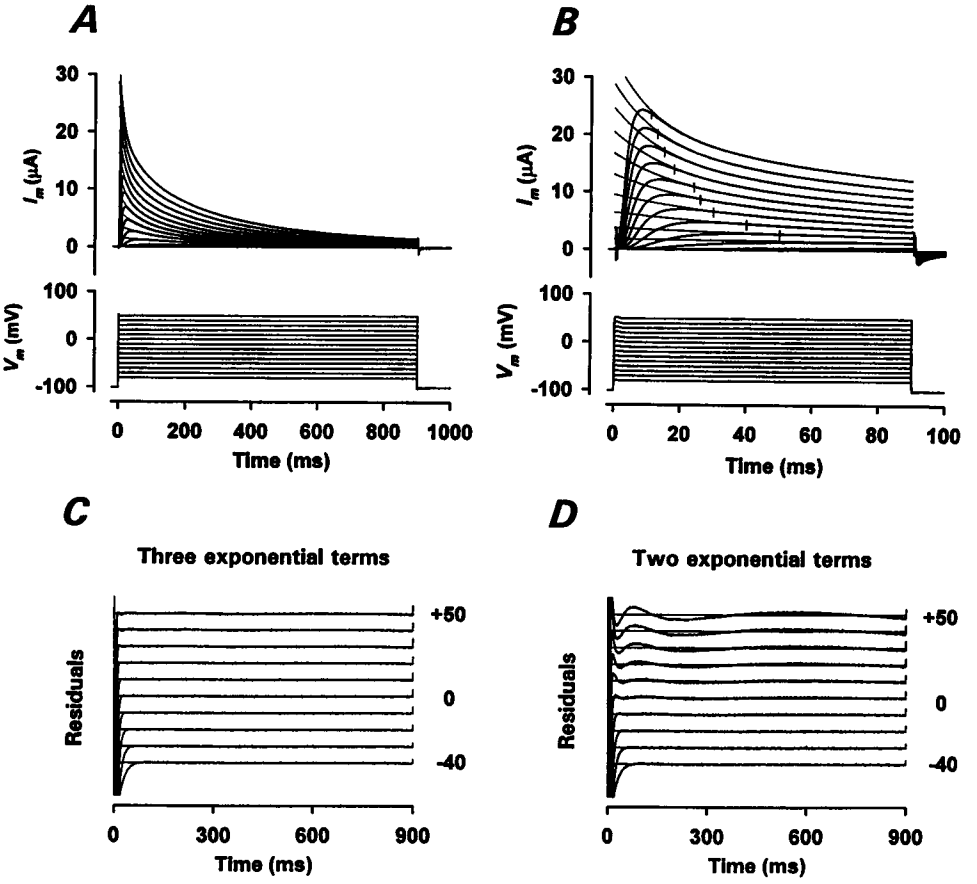

FIGURE 1 Macroscopic inactivation kinetics of mKv4.1 K^+ channels expressed in *Xenopus* oocytes. (*A*) *Upper panel:* Whole-oocyte currents elicited in response to 900-ms step depolarizations from a holding potential of −100 mV to test potentials from −80 to +50 mV in increments of 10 mV. The interpulse interval was 5 s. Thin lines superimposed on current traces represent best fits to the sum of three exponential terms (−10 to +50 mV), the sum of two exponential terms (−30 and −20 mV) and a single exponential term (−40 mV). Best-fit parameters are shown in Fig. 2. *Lower panel:* Corresponding recording of membrane potential. Note stability during pulse. (*B*) Whole-oocyte currents elicited in response to 90-ms step depolarizations, otherwise as described in *A*. Families of traces in *A* and *B* are from the same oocyte. Small vertical marks represent cursor position (see Materials and Methods). (*C* and *D*) Residuals of multiexponential fits (sum of two or three exponential terms) for currents shown in *A* and *B*. For clarity, residuals at different membrane potentials in *C* and *D* were shifted arbitrarily by 2 μA.

decay of the current was not significantly affected by uncompensated series resistance, which is confirmed by the presence of a stable voltage during step depolarizations (Fig. 1, *A* and *B*). In addition, similar results were obtained with cell-attached macropatches (not shown).

N- and C-terminal deletions in mKv4.1 produce similar effects on the kinetics of macroscopic currents

To examine the contribution of the N-terminus to rapid inactivation in mKv4.1, we created a deletion mutant that eliminated 70 amino acids at the N-terminus (Δ2-71; Fig. 3). An earlier characterization of mKv4.1 reported that deletion of 31 amino acids at the N-terminus (Δ2-32) inhibited the fast component of macroscopic inactivation, slowed the rising phase of the current, and delayed time to peak (Pak et al., 1991). In our study we found that at positive membrane potentials Δ2-71 caused similar effects (Fig. 4). Thus, in the absence of residues 2–32, the next 39 residues do not seem to play a significant additional role on current kinetics (see below). These results suggested that a region within the first 32 amino acids influences rapid current inactivation and the current's rising phase.

The N-terminal region of Shal K^+ channels is highly conserved (Baldwin et al., 1991; Baro et al., 1996; Pak et al., 1991; Serodio et al., 1996). For instance, positions 1–19 include mostly nonpolar amino acids and a conserved, positively charged amino acid (Arg) at position 13; other conserved regions include positions 26–37 and 45–68. Deletion of a triad of basic amino acids (Δ35-37, eliminating R35, K36, and R37; R = Arg, K = Lys) at the N-terminus of rKv4.2 slowed rapid inactivation (Baldwin et al., 1991). However, no effect was observed when R35 or K36 was mutated to glutamine (Q). In agreement with this result, a double mutant affecting homologous residues in mKv4.1 (K34Q/R37Q) did not affect macroscopic current kinetics (Fig. 4). Similarly, R13Q caused little or no effect on current kinetics (Fig. 4). Because Δ2-32 had already eliminated most of the hydrophobic N-terminal region (Pak et al., 1991), Δ2-72 caused no additional kinetic alterations. Thus, rapid inactivation in Shal K^+ channels requires a sequence of mostly hydrophobic amino acids at the N-terminus, and the charge of adjacent basic amino acids does not seem to play a significant role. The effect of Δ35-37 in rKv4.2 may have simply been caused by a shortening of the N-terminus (see Discussion).

Because currents expressed by mKv4.1 N-terminal deletions retained their transient nature (Fig. 4), we decided to investigate whether other putative cytoplasmic regions may also contribute to the inactivation of mKv4.1. We created a series of C-terminal deletions (Fig. 3): Δ556-651 (the last 96

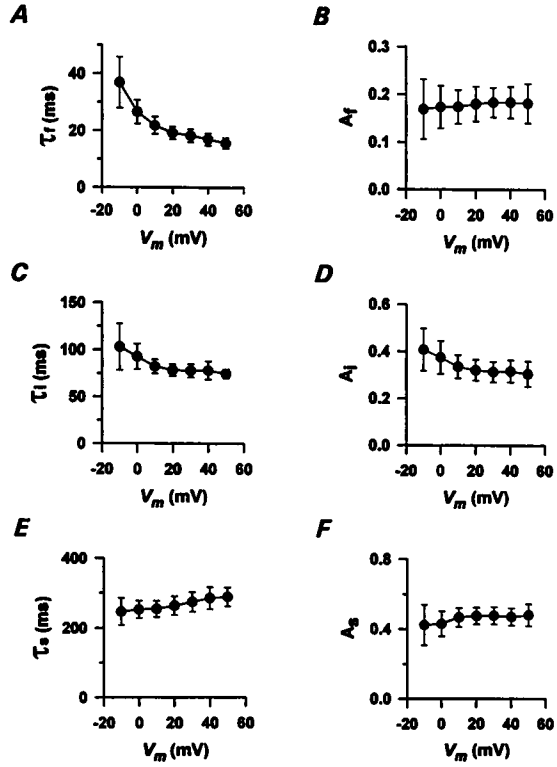

FIGURE 2 Voltage dependence of kinetic parameters of macroscopic inactivation. Time constants and fractional amplitudes were obtained from fitting the sum of three exponential terms to the decay phase of the current (Fig. 1). τ_f, τ_i, and τ_s represent fast, intermediate, and slow time constants, respectively. A_f, A_i, and A_s represent the corresponding relative magnitudes of the exponential terms. Symbols and bars represent the mean ± SD (n = 16). The steady-state level of the current ($a\infty$) ranged between 2% and 4% of total decay and was weakly voltage dependent.

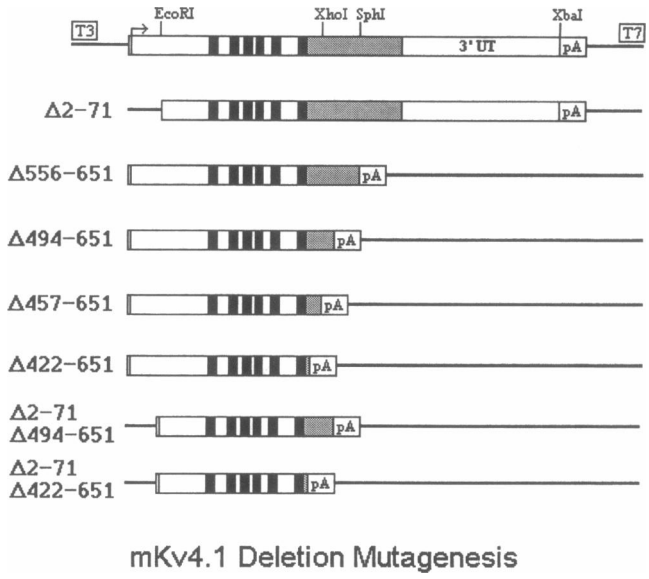

FIGURE 3 Deletion mutagenesis of mKv4.1. Schematic representation of wild-type and mutant constructs. Boxed areas represent the mKv4.1 insert in pBluescript KS II. Membrane-spanning domains (S1–S6) are represented by black bars. The hydrophilic C-terminus (down to the stop codon) is shaded gray. 3'UT represents the 3' untranslated region. A polyadenylated tail (A_{32}) is represented as pA.

residues), Δ494-651 (the last 158 residues), Δ457-651 (the last 195 residues), and Δ422-651 (the last 230 residues). Δ422-651 removes all but 13 amino acids at the hydrophilic C-terminus. We also created two double deletions affecting both N- and C-terminal domains: Δ2-71/Δ494-651 and Δ2-71/Δ422-651, but only the first expressed functional currents. The cumulative net charge removed increases with progressively longer deletions at the C-terminus. Assuming that arginine or lysine contributes +1, glutamate or aspartate contributes −1 and histidine contributes +0.5, the net charge removed is −1.5, +3.5, +4.0, and +11.0 for Δ556-651, Δ494-651, Δ457-651, and Δ422-651, respectively. Large charge changes occur between Δ556-651 and Δ494-651, and between Δ457-651 and Δ422-651. Δ556-651 caused few or no apparent functional alterations (Figs. 4–7 and Table 1), whereas larger C-terminal deletions affected current kinetics and voltage-dependent properties in a manner that resembled the effect of deletions at the N-terminus (Figs. 4–7 and Table 1). These results indicated that domains at the N-terminus and the C-terminus are functionally equivalent and predict that a double deletion affecting both termini should exhibit no additivity. Indeed, Δ2-71/Δ494-651 expressed currents that were similar to those observed with Δ2-71 or Δ494-651 alone (Fig. 4 and Table 1). The similarity between the effects of N- and C-terminal deletions cannot be exclusively attributed to the net charge removed because Δ2-71 removed +1, and all C-terminal deletions that mimicked the effects of Δ2-71 caused a significantly larger net change of charge. Rapid inactivation gating in mKv4.1 might result from the concerted action of N- and C-terminal domains.

The fast component of macroscopic inactivation is absent in most N- and C-terminal deletion mutants

By contrast to wild type, whole-oocyte currents expressed by most deletion mutants exhibited a decay that was fitted very well by the sum of two exponential terms (Δ556-651 was nearly indistinguishable from wild type; Fig. 4). This is illustrated in Fig. 5 for Δ2-72 and Δ422-651. The values of the two time constants were, in fact, similar to those of the intermediate and slow components observed with wild-type currents, and showed little or no voltage dependence between −10 and +50 mV (Fig. 5, *C* and *D*). The largest difference was observed with Δ422-651 (see below). Fig. 6 shows that, except for Δ556-651, all deletion mutants studied here eliminated the fast time constant of current decay. Fractional amplitudes of the exponential terms (A_s, A_i) were voltage independent (not shown). Analysis of the ratio A_s/A_i (at +50 mV) revealed, however, that for Δ494-651, Δ457-651, Δ2-71, and Δ2-71/Δ494-651 this variable increased significantly above wild-type value (Fig. 6 *B*, *upper panel*). In addition, deletion mutants that eliminated part of the

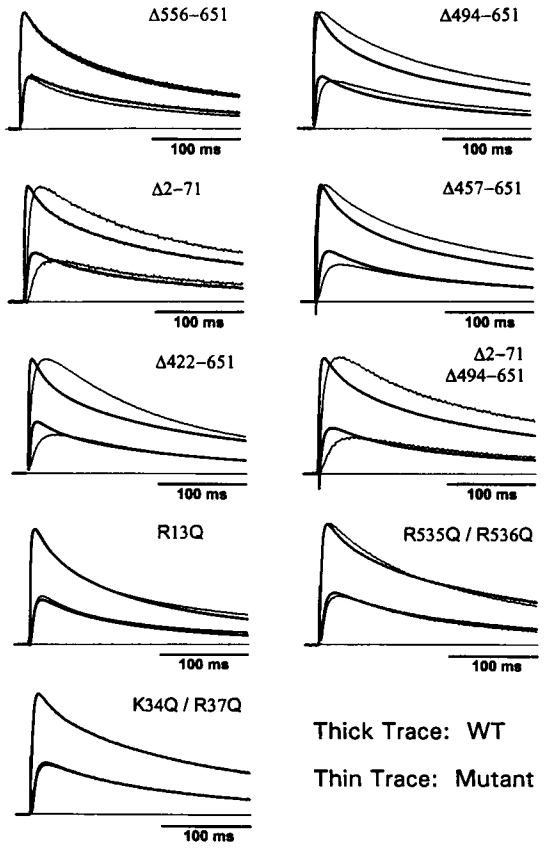

FIGURE 4 Effects of mutations at the cytoplasmic N- and C-terminal domains of mKv4.1. Currents were elicited by a step depolarization to 0 and +50 mV from a holding potential of −100 mV. For comparison, currents are shown normalized and superimposed (peak current at +50 mV for each pair). Each set of currents was recorded from the same batch of oocytes. Peak currents (in μA) at +50 mV were as follows for Δ556-651, Δ2-71, Δ494-651, Δ457-651, Δ422-651, Δ2-71/Δ494-651, R13Q, K34Q/R37Q and R535Q/R536Q (wild-type/mutant): 1.2/1.5, 1.6/0.9, 31.8/5.3, 4.8/3.9, 31.8/3.7, 6.5/1.5, 30.1/23.5, 11.5/11.3, 11.6/5.8, respectively.

N-terminus (Δ2-71 and Δ2-71/Δ494-651) also increased the magnitude of the steady-state level of the current (Fig. 6 *B*, *lower panel*). Δ422-651 was apparently an exception. This mutant slightly reduced the ratio A_s/A_i and did not affect the steady-state level of the current at depolarized voltages (Fig. 6 *B*). Nevertheless, Δ422-651 exhibited a significantly slower intermediate time constant, which completely lacked voltage dependence between −10 and +50 mV (Fig. 5 *C*). These results showed that both N- and C-terminal deletions (except Δ556-651) selectively abolished rapid macroscopic inactivation (or it can no longer be resolved). Current decay was further slowed by changes that affected later kinetic components. Therefore, rapid inactivation in mKv4.1 seemed partially coupled to slower inactivation processes.

N- and C-terminal deletions caused a similar loss of voltage dependence

Inspection of traces shown in Fig. 4 reveals that at 0 mV N- and C-terminal deletions that abolished rapid inactivation also caused a slower rising phase and reduced peak (when currents are normalized at +50 mV). These changes suggested altered voltage-dependent gating. To further examine this possibility, we analyzed the conductance-voltage relationship and voltage dependence of prepulse inactivation at steady state (Table 1). N- and C-terminal deletions that eliminated rapid inactivation significantly increased the slope factor (s_a) without affecting the midpoint potential (V_a) for activation of one subunit (Table 1). The midpoint potential of prepulse inactivation (V_h) was not significantly affected by C-terminal deletions (Table 1). However, Δ2-71 and Δ2-71/Δ494-651 exhibited a moderate depolarizing shift (8 and 4 mV, respectively). In agreement with the analysis of conductance-voltage curves, all deletion mutants that abolished rapid inactivation also displayed reduced voltage dependence of prepulse inactivation (s_h increases, Table 1). Qualitatively, these results are also in agreement with a reduced voltage dependence of inactivation, especially apparent with Δ422-651 (Fig. 6). Mutants that altered voltage-dependent gating also exhibited increased 50% rise time (1.5- to 2-fold at +50 mV; Fig. 4 and Table 1). This might have resulted from a combination of two effects: 1) elimination of rapid inactivation (channels that were yet to open during the early part of a depolarizing pulse would now contribute more to the current); and 2) reduced voltage dependence of activation (spreading the effect of membrane potential on the rising phase of the current; Fig. 1 *B*).

N- and C-terminal deletions also affected recovery from inactivation

In general, wild-type mKv4.1 and deletion mutants exhibited time courses of recovery from inactivation (at −120, −100, and −80 mV) that were well described as an exponential rise (Fig. 7 *A* and *legend*). Kinetic analysis of current decay and selective elimination of the rapid component of current decay by N- and C-terminal deletions suggested, however, the presence of more than one inactivated state (Figs. 1 and 5). This apparent discrepancy can occur when kinetic components corresponding to the recovery from multiple inactivated states cannot be resolved (e.g., time constants of recovery may not differ by more than twofold). Comparison of the time constants of recovery from inactivation revealed that Δ2-71 and Δ422-651 caused little change at −120 and −100 mV, but significant acceleration at −80 mV (Fig. 7). A semilogarithmic plot of time constants of recovery from inactivation against membrane potential (Fig. 7 *B*, Δ2-71 and Δ422-651) showed reduced voltage dependence. This is in agreement with reduced voltage-dependent gating (Table 1). By contrast, Δ494-651 and Δ2-71/Δ494-651 exhibited significantly slower recovery from inactivation at all membrane potentials tested (Fig. 7). These mutants and wild-type exhibited parallel voltage dependence of the time constants of recovery from inactivation (Fig. 7 *B*). In short, the longest C-terminal deletion

TABLE 1 Parameters of macroscopic activation and inactivation

	Wild type	Δ2–71	Δ556–651	Δ494–651	Δ457–651	Δ422–651	Δ2–71/Δ494–651
V_a[a](mV)	−49 ± 2	−48 ± 3	−52 ± 2	−52 ± 3	−52 ± 6	−50 ± 3	−51 ± 5
s_a[a](mV/*e*-fold)	22.3 ± 0.4	26.5 ± 1.3*	21.1 ± 0.8†	27.0 ± 1.0*	28.7 ± 2.3*	32.1 ± 1.4*	26.4 ± 1.5*
(*n*)[a]	(7)	(8)	(6)	(10)	(3)	(5)	(7)
V_h[b](mV)	−69 ± 2	−61 ± 3	−69 ± 2	−70 ± 1	−69 ± 2	−71 ± 2	−65 ± 4
s_h[b](mV/*e*-fold)	5.0 ± 0.4	6.5 ± 0.2**	5.8 ± 0.6††	5.7 ± 0.5**	6.2 ± 0.5**	6.4 ± 0.4**	6.4 ± 0.5**
(*n*)[b]	(6)	(3)	(3)	(8)	(3)	(4)	(6)
$t_{0.5}$[c](ms)	2.4 ± 0.5	4.6 ± 0.3*	1.7 ± 0.1*†	3.7 ± 0.6*	3.7 ± 0.1*	4.3 ± 0.6*	5.2 ± 0.4*
(*n*)[c]	(4)	(6)	(4)	(7)	(3)	(5)	(9)

[a]Values corresponding to the activation parameters obtained from the G_p-V curve. Peak conductance was calculated as $G_p = I_p/(V - V_r)$, where I_p is the peak current, V is command voltage, and V_r is the reversal potential (−90 to −95 mV). $G_p - V$ curves were well described assuming a fourth-order Boltzmann distribution. $G_p = G_{pmax}/[1 + \exp(V_a - V)/s_a]^4$, where G_{pmax} is the maximum peak conductance, V_a is the midpoint voltage for activation of one subunit, and s_a is the slope factor. All values in this table are presented as means ± SD from *n* independent determinations (in parentheses).

[b]Values corresponding to the inactivation parameters obtained from prepulse inactivation experiments (*h*-infinity). $I_p - V$ curves were well described assuming a simple Boltzmann distribution. $I_p = I_{pmax}/[1 + \exp(V - V_h)/s_h]$, where I_{pmax} is maximum peak current, V_h is the midpoint voltage of the distribution, V is prepulse voltage, and s_h is the slope factor.

[c]This value represents the 50% risetime of the current at +50 mV.

*$P < 0.007$. **$P < 0.015$. $^{\dagger}P = 0.005$. $^{\dagger\dagger}P = 0.044$. *$^{\dagger}P = 0.022$. All *P* values were determined relative to wild type by a two-tailed Student's *t*-test.

(Δ422-651) and Δ2-71 altered recovery by reducing its voltage dependence. A shorter deletion (Δ494-651), on the other hand, simply retarded recovery from inactivation (Δ457-651 behaved similarly; not shown). This effect was dominant when Δ494-651 is combined with Δ2-71 (suggesting that Δ494-651 compensates the effect of Δ2-71 on voltage dependence of recovery from inactivation). Overall, these results show that the N-terminus and the hydrophilic C-terminal domain exert significant influence on recovery from inactivation. Furthermore, as indicated before, a C-terminal deletion (Δ422-651) can mimic the effect of a deletion at the N-terminus (Δ2-71).

Discrete mutations affecting charged residues at the N- and C-terminal domains inhibited functional expression of mKv4.1

In examining the primary sequence of the termini in mKv4.1, we found a net negative charge at the N-terminus (charge density increases sharply downstream from residue at position 30). By contrast, the hydrophilic C-terminus is highly basic, especially within a region of 30 amino acids that follows the sixth transmembrane domain. A net positive charge is maintained between residues 412 and 570. The rest of the polypeptide toward the C-terminus is less charged and mostly neutral (total length of the mKv4.1 polypeptide is 651 residues). A similar pattern is conserved in rKv4.2, rKv4.3, and *Drosophila* homologs Shal1 and Shal2 (Baldwin et al., 1991; Pak et al., 1991; Baro et al., 1996; Serodio et al., 1996) but is not found in ShakerB, Kv1.4, or Kv3.4 (three distinct A-type K^+ channels). Given an opposite distribution of charges at the termini of Shal channels, it can be suggested that the termini may interact through electrostatic interactions. To determine the residues that may contribute, we created the following mutations affecting an acidic triplet at the N-terminus and two basic pairs at the C-terminus: D115N/E116Q/E117Q, R535Q/R536Q, and R539Q/R540Q (D = Asp, E = Glu). These basic pairs were selected because they were included in the most distal deletion that caused a significant functional effect (Δ494-651) and near the end of the positively charged region at the C-terminus. Whereas R535Q/R536Q produced functional currents (5.2 ± 3.6 μA, $n = 5$) exhibiting a time course of rapid inactivation that seemed slightly slower than wild type (Figs. 4 and 6), it was surprising to find that mutation of the acidic triplet (D115N/E116Q/E117Q) at the N-terminus or a basic pair at the C-terminus (R539Q/R540Q) nearly abolished functional expression (≥99% inhibition). When we used two batches of oocytes and similar amounts of cRNA (75 ng/oocyte), the average peak currents at +50 mV were 18 ± 10 μA ($n = 8$), 0 μA ($n = 10$), and 0.09 ± 0.07 μA ($n = 7$) for wild type, D115N/E116Q/E117Q, and R539Q/R540Q, respectively. These results were confirmed with two more sets of mutant cRNA and two more batches of oocytes. Mutants did not express even when we injected fourfold more concentrated cRNA (~280 ng/oocyte). The mutations could not be functionally rescued by coexpression with wild type. However, dominant suppression was observed with R539Q/R540Q only. These results were surprising because deletion of most of the C-terminus was tolerated (Figs. 3 and 4). However, if N- and C-terminal domains interact at specific points, discrete mutations that inhibited functional expression may have caused a mismatch between the termini, leading to significant structural distortion and, consequently, unstable subunit assembly or a nonfunctional conformation. Thus a close interaction between the termini may be critical for the functional stability of the intact channel oligomer and may be required for rapid channel inactivation.

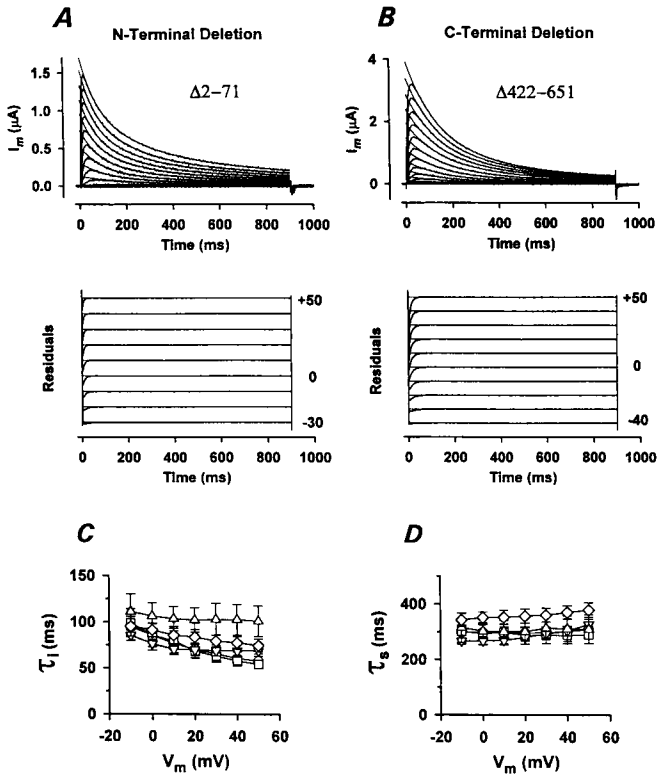

FIGURE 5 Inactivation kinetics of mKv4.1 mutants. (*A*) Whole-oocyte currents expressed by Δ2-71. Currents were elicited in response to 900-ms step depolarizations from a holding potential of −100 mV to test potentials from −80 to +50 mV in increments of 10 mV. The interpulse interval was 10 s. Thin lines superimposed on current traces represent the best fit to the sum of two exponential terms (Materials and Methods). The lower part shows the residuals of such fits. For clarity, the residuals at different membrane potentials have been shifted arbitrarily by 1 μA. (*B*) Whole-oocyte currents expressed by Δ422-651. Recording and fits as in *A*. (*C*) Voltage dependence of τ_i. Although currents are described by two exponential terms, the fast time constant is named τ_i because its magnitude and voltage dependence are similar to those of τ_i from wild-type channels (see text). ○, Δ494-651; □, Δ457-651; △, Δ422-651; ▽, Δ2-71; ◇, Δ2-71/Δ494-651. (*D*) Voltage dependence of τ_s. The amplitudes of the exponential terms exhibited no voltage dependence.

The inactivation gate of mKv4.1 K^+ channels may not behave like a simple open-channel blocker

In light of the results presented in previous sections, it seemed apparent that the molecular mechanism of rapid inactivation of mKv4.1 K^+ channels may differ from that demonstrated for ShakerB K^+ channels. To further examine that possibility, we tested the effects of internal and external TEA on peak current and current decay and the effect of an elevated external K^+ concentration on the rate of recovery from inactivation (Fig. 8). If TEA and the N-terminal inactivation "ball" act as pore blockers and share a common receptor at the inner mouth of the pore, macroscopic inactivation should be retarded by TEA in a manner that is quantitatively proportional to the degree of TEA-induced block (Choi et al., 1991). We found that internal application of 5 mM TEA to the cytoplasmic side of inside-out patches caused significant inhibition of the peak current (50–60%) but did not greatly affect the time constant of rapid inactivation (Fig. 8, *A* and *C*). A similar result was obtained when TEA was injected into intact oocytes (not shown). Alternatively, mKv4.1 K^+ channels may undergo C-type inactivation. Binding of TEA to an external site near the outer mouth of ShakerB K^+ channels directly interferes with that process (see Introduction) and thus slows down C-type inactivation (Choi et al., 1991). We found that 96 mM external TEA weakly inhibited mKv4.1 currents (~30%), causing little or no effect on current kinetics (Fig. 8, *B–C*). Finally, elevation of external K^+ concentration accelerates recovery from inactivation in ShakerB K^+ channels (Demo and Yellen, 1991). In such a case, pore blockade by the N-terminal domain is relieved by incoming K^+ ions. Contrary to that result, we found that 98 mM external K^+ retarded recovery from inactivation in mKv4.1 K^+ channels (Fig. 8 *D*). Moreover, macroscopic inactivation occurred at a faster rate and, once the current had inactivated, no large tail currents with slow kinetics were observed upon repolarization (Fig. 8 *C*, *inset*). A large tail current with slow kinetics is expected to occur if inactivated channels reopen during recovery from inactivation (Demo and Yellen, 1991; Ruppersberg et al., 1991). Overall, these results suggest that mKv4.1 K^+ channels do not undergo N- and C-type inactivation, as known in ShakerB K^+ channels.

DISCUSSION

We have investigated the structural basis of rapid inactivation gating in a neuronal A-type K^+ channel encoded by mKv4.1. Our main results and conclusions are summarized below: 1) Inactivation of whole-oocyte currents at positive membrane potentials exhibited a nonexponential time course. The sum of at least three exponential terms was necessary to describe current decay with time constants that differed by fourfold or more between them (Figs. 1 and 2). 2) Mutagenesis of the hydrophilic C-terminal region of the polypeptide revealed that deletion of 96 amino acids had no effect, but longer deletions (158, 195, and 230 amino acids) caused loss of rapid current inactivation with some effect on slower components of the current (mainly affecting the relative amplitudes of slower terms and the steady-state current). A very similar result was observed when we deleted 70 amino acids at the N-terminus (Figs. 3–6). Furthermore, simultaneous deletion of 70 residues at the N-terminus and 158 at the C-terminus exhbited no additivity or additional affects. 3) All deletion mutants that affected inactivation reduced voltage dependence (as determined from the Gp-V curve and prepulse inactivation at steady state) and slowed the rising phase of the macroscopic current (Table 1). 4) Deletion mutants that affected rapid inactivation also altered recovery from inactivation (Fig. 7). 5) Observations with TEA and an increased external K^+ concentration did not support the presence of N-type or C-type inactivation in mKv4.1 K^+ channels (Fig. 8). These

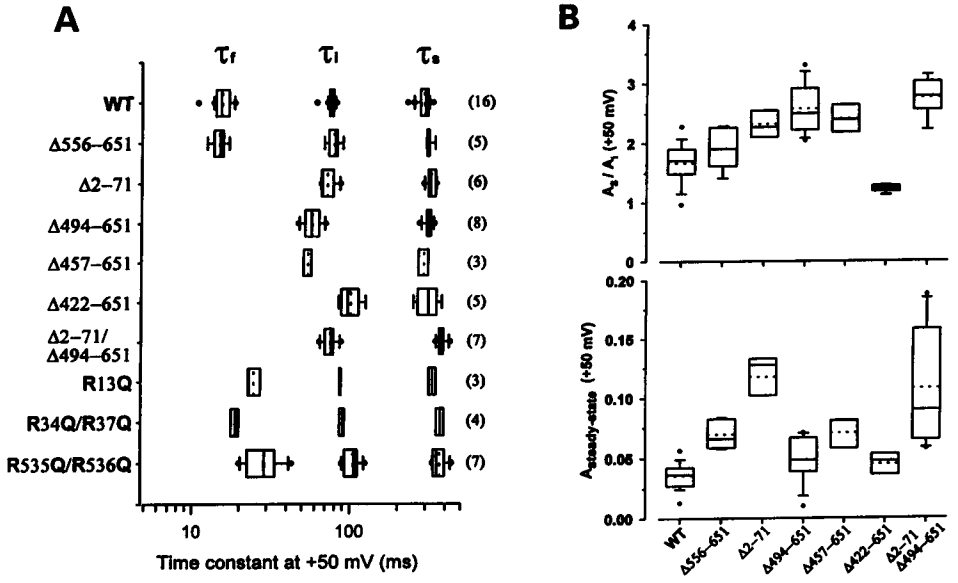

FIGURE 6 Kinetic parameters of inactivation of wild-type mKv4.1 and various mutants at +50 mV. (*A*) Tukey box plot summarizing the values of the time constants of inactivation at +50 mV (see Figs. 1, 2, and 5). The number of independent determinations is indicated by the figures in parentheses. (*B*) Tukey box plots summarizing the values of the ratio A_i/A_s and the steady-state current. Horizontal lines of a box represent 25th, 50th, and 75th percentile points. Dashed line represents the mean value. Whiskers represent 10th and 90th percentile points and symbols indicate outliers.

data demonstrate a novel role of the hydrophilic C-terminal domain of K^+ channels as a structural component necessary to maintain rapid inactivation gating. In addition, we found that mutations that eliminated negatively charged residues at the N-terminus (D115, E116, E117) or positively charged residues at the C-terminus (R539, R540) virtually abolished functional expression. This result suggested that acidic residues at the N-terminus and basic residues at the C-terminus might specifically interact with each other. The mechanism and consequences of this putative interaction are discussed later.

The inactivation gate and the nature of rapid inactivation in mKv4.1 K^+ channels

Two sets of observations support the notion that an amphipathic region at the N-terminus of mKv4.1 is the main component of the inactivation gate: 1) deletions within this domain slow or abolish rapid current inactivation (Baldwin et al., 1991; Pak et al., 1991; and this study); and 2) although there is little sequence homology among the N-terminal domains of other K^+ channels that undergo rapid inactivation (e.g., ShakerB, Kv1.4, and Kv3.4), all share an amphipathic region that is the main determinant of rapid inactivation gating in these channels (e.g., Murrell-Lagnado and Aldrich, 1993a,b). The equivalent region in mKv4.1 is also highly divergent when compared to those channels, but an amphipathic sequence is also found here. The first 30 residues at the N-terminus of the mKv4.1 polypeptide are mostly hydrophobic. If this domain constitutes the inactivation gate in mKv4.1 K^+ channels, do they undergo "ball-and-chain" N-type inactivation like Shaker K^+ channels? Our results with internal TEA and a high external K^+ concentration (Fig. 8) demonstrate that mKv4.1 K^+ channels do not undergo N-type inactivation, as shown in Shaker K^+ channels. Supporting this conclusion, we also reported here that several basic amino acids at the N-terminus (R13, K34, and R37) do not seem to contribute to current inactivation. This implies that TEA and the cytoplasmic inactivation gate of mKv4.1 K^+ channels do not share the same internal receptor, and rapid inactivation of these channels does not require a positively charged blocking particle. C-type inactivation also seems unlikely because external TEA had little effect on current decay (Fig. 8). In addition, the mutations that we studied here affected rapid inactivation but do not include residues that are presumably involved in C-type inactivation, namely amino acids in the P-region (S5-S6 linker) and S6 (Hoshi et al., 1991; Lopez-Borneo et al., 1993). Specially interesting is threonine at position 449 in the P-region of ShakerB. Mutation of this residue to valine causes nearly complete elimination of C-type inactivation, and mutation to alanine, lysine, glutamine, or serine dramatically speeds it up (Lopez-Borneo et al., 1993). Because the equivalent position in mKv4.1 is occupied by valine, it indeed seems unlikely that the processes that we have studied here are related to C-type inactivation, as shown in Shaker K^+ channels. Furthermore, our results demonstrated that mKv4.1 do not recover through the open state and incoming K^+ ions seem to stabilize the inactivated state (Fig. 8). Thus if channels have to close first before they recover from inactivation, K^+ ions occupying a putative pore site may delay closing of inactivated channels, causing slower recovery from inactivation (closing of open channels, however, was not affected by an elevated external K^+ concentration). Thus it appears that rapid inactivation of mKv4.1 K^+ channels may involve a distinct mechanism that probably utilizes a mostly hydrophobic domain at the N-terminus as an inactivation gate in combination with novel elements that function in a unique way.

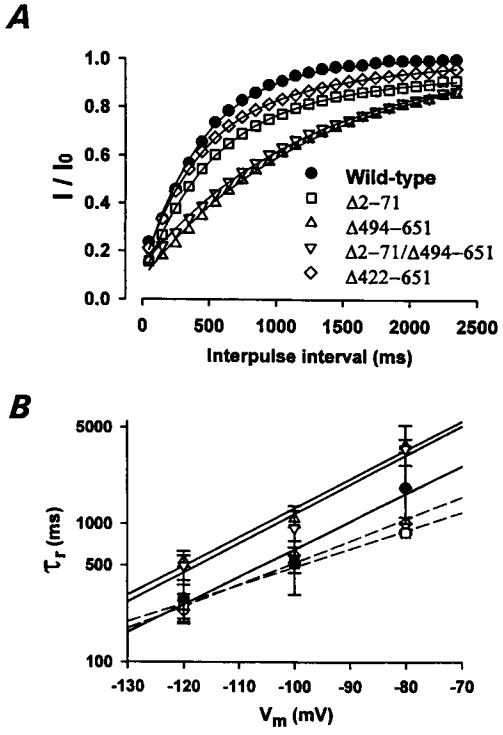

FIGURE 7 Recovery from inactivation of wild-type mKv4.1 and various deletion mutants. (*A*) Recovery from inactivation at −100 mV. A double-pulse protocol was used to measure the time course of recovery from inactivation. The first pulse (control) inactivated >80% of the current at +40 mV. During a variable interpulse interval the membrane potential was held at −100 mV. The second pulse (at +40 mV) tested the magnitude of the current that recovered during the interpulse interval. Data were plotted as peak current obtained in response to the second pulse divided by the control peak current (I/I_0) against the interpulse interval. Solid lines represent the best fits assuming an exponential time course. Time constants were 467 ms, 574 ms, 1251 ms, 1247 ms, and 535 ms for wild-type, Δ2-71, Δ494-651, Δ2-71/Δ494-651, and Δ422-651, respectively. (*B*) Voltage dependence of the time constants of recovery from inactivation (points represent the mean ± SD, n = 3–7). Regression lines through the points gave the following slopes (mV/*e*-fold): 14, 24, 13, 13, and 21 for wild-type, Δ2-71 (*dashed line*), Δ494-651, Δ2-71/Δ494-651, and Δ422-651 (*dashed line*), respectively. Δ2-71 required the sum of two exponential terms to describe its recovery from inactivation at −120 mV. Only the fast time constant (which represents ~2/3 of the time course) is plotted here. The slow time constant was 980 ± 341 ms.

The hydrophilic C-terminal domain, a novel component of the inactivation machinery of K^+ channels

One of the most remarkable findings of our study was that C-terminal deletions could mimic the effect of N-terminal deletions on inactivation and gating. Moreover, a double N- and C-terminal deletion did not cause significant additional effects. Thus we reasoned that 1) the hydrophilic C-terminus, which is highly basic and probably cytoplasmic, is an essential part of the molecular apparatus that controls rapid inactivation in mKv4.1, and 2) a simple interpretation of our results should incorporate interactions between the termini of the channel polypeptide or between the termini and a rate-limiting domain that controls rapid inactivation gating. Given the results from C-terminal deletions, it is conceivable that a domain at the C-terminus might be the actual inactivation gate. However, mainly because the mKv4.1 polypeptide has a hydrophobic N-terminal domain analogous to that found at the N-terminus of rapidly inactivating K^+ channels (see above), we prefer to suggest that C-terminus in mKv4.1 serves to position and maintain the N-terminal inactivation gate in close proximity to the inner mouth of the pore. This implies that part of the C-terminus may form part of the cytoplasmic vestibule of the channel and interact with the N-terminus (see below). Consistent with the idea of proximity between the termini and the core of the channel, we found that deletions that affected inactivation also altered voltage dependence (Table 1). Thus the termini may also interact with parts of the voltage sensor (S4 and the S4-S5 loop) and contribute to coupling between activation and inactivation in mKv4.1. This is reminiscent of a similar interaction involving the linker between domains III and IV of voltage-gated Na^+ channels (O'Leary et al., 1995) and a possible interaction between the N-terminus and the gating machinery of HERG channels (Spector et al., 1996). In Shaker K^+ channels it has been found that long-range electrostatic interactions involving basic residues at the N-terminus may bring the inactivation "ball" near the inner mouth of the pore (Murrell-Lagnado and Aldrich, 1993a). An important consequence of a preexisting close proximity between the inactivation gate and the pore is that long-range electrostatic interactions may not be necessary to control the rate of inactivation in mKv4.1. In fact, we found that basic residues at positions 13, 34, and 37 do not contribute significantly to rapid current inactivation. Moreover, if the position of the gate is critical, a short internal deletion at the N-terminus should disrupt rapid inactivation. Accordingly, Baldwin et al. found that deletion of three residues (R35, K36, and R37) significantly retarded rapid inactivation of rKv4.2 (a rat Shal homolog), whereas mutation of two of these residues to glutamine had no effect (Baldwin et al., 1991). Similarly, basic amino acids adjacent to the hydrophobic inactivation domain in voltage-gated Na^+ channels do not seem to be critical determinants of rapid inactivation (West et al., 1992).

What kind of interactions help to position the inactivation gate in mKv4.1? Because a large domain downstream from the inactivation gate (positions 60–160) exhibits clusters of acidic amino acids and a net negative charge (−13), and two domains at the C-terminus (positions 420–450 and 510–556) exhibit clusters of basic amino acids and net positive charges (+9 and +8, respectively), it is possible that electrostatic interactions between these domains help to position and/or maintain the inactivation gate near the inner mouth of the pore. Is this a stable interaction involving salt bridges (structural hypothesis), or a long-range reversible interaction that takes place during channel activation (functional hypothesis)? Because mutation of critical acidic residues at the N-terminus or basic residues at the C-terminus greatly inhibited functional expression (see Results), we favor the

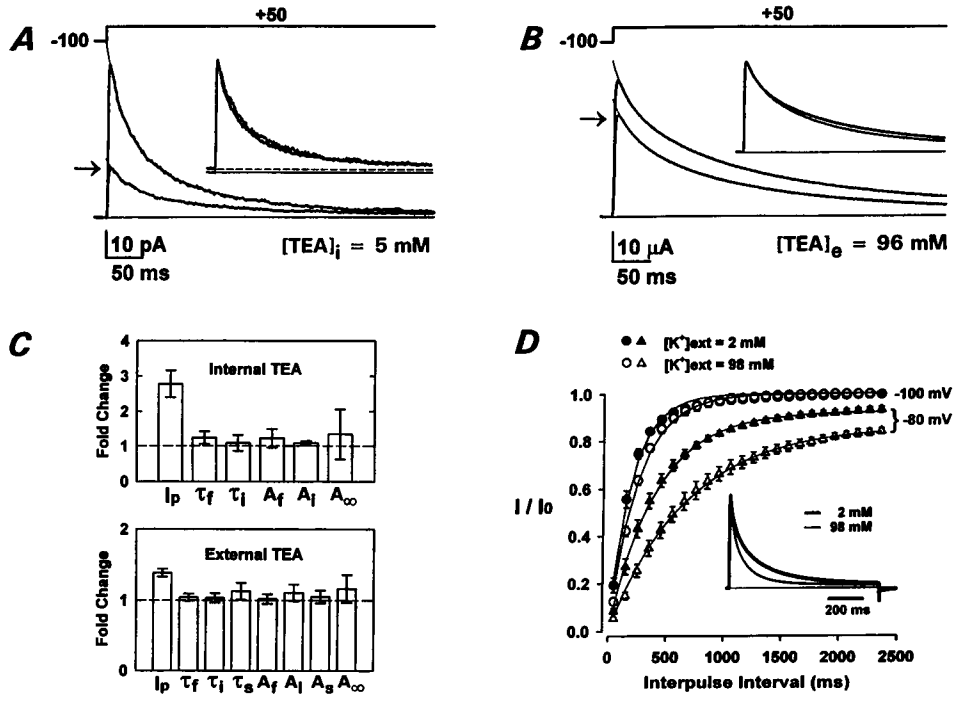

FIGURE 8 The effects of TEA and external K^+ on inactivation of mKv4.1 K^+ channels. (*A*) Inhibition of the mKv4.1 outward current by application of 5 mM TEA to the cytoplasmic side of an inside-out membrane patch. Arrow indicates the trace recorded in the presence of TEA. Although whole-oocyte currents are well described by the sum of three exponential terms (Fig. 1), currents recorded from inside-out patches exhibited a greatly reduced slow component of macroscopic inactivation (E. Beck, H. Jerng, and M. Covarrubias, unpublished observations). A thin line superimposed on the decaying phase of the traces represents the best fit, assuming the sum of two exponential terms. Control best-fit parameters were τ_f = 22 ms, τ_i = 108 ms, A_f = 0.44, A_i = 0.53, A_∞ = 0.03. Best-fit parameters in the presence of TEA were τ_f = 27 ms, τ_i = 116 ms, A_f = 0.40, A_i = 0.54, and A_∞ = 0.06 (for definitions, see *C*). The inset shows a direct comparison of current kinetics by scaling up the trace recorded in the presence of TEA. A trace offset was necessary to compensate for a small difference in the steady-state current level (*dashed line*). (*B*) Inhibition of the mKv4.1 outward current by external application of 96 mM TEA in the whole-oocyte mode. Arrow indicates the trace recorded in the presence of TEA. A thin line superimposed on the decaying phase of the traces represents the best fit, assuming the sum of three exponential terms. Control best-fit parameters were τ_f = 17 ms, τ_i = 83 ms, τ_s = 292 ms, A_f = 0.15, A_i = 0.30, A_s = 0.53, A_∞ = 0.02. Best-fit parameters in the presence of TEA were τ_f = 19 ms, τ_i = 85 ms, τ_s = 257 ms, A_f = 0.14, A_i = 0.37, A_s = 0.47, A_∞ = 0.02 (for definitions, see *C*). Inset as described above, but no trace offset was necessary. (*C*) Bar graphs summarizing the effects of internal and external TEA on mKv4.1 outward currents at +50 mV. Estimated parameters are expressed as fold change relative to control. I_p represents the peak current. Kinetic parameters τ_f, τ_i, τ_s, A_f, A_i, A_s, and A_∞ represent time constants and fractional amplitudes as described in Fig. 2, legend. Values are expressed as mean ± SD (internal TEA, n = 4; external TEA, n = 3). (*D*) The effect of high external K^+ on recovery from inactivation at −100 and −80 mV (for description of voltage-clamp protocol see Fig. 7). Line through the points (mean ± SD, n = 4) represents the best fit, assuming a simple exponential rise. Time constants at −100 mV were 195 and 252 ms in 2 and 98 mM external K^+, respectively. Time constants at −80 mV were 400 and 660 ms in 2 and 98 mM external K^+, respectively. The inset demonstrates the effect of high external K^+ on the kinetics of the whole-cell current at +50 mV. Trace obtained in the presence of 98 mM K^+ was scaled up (×1.7) to match peak current. All data for *C* were obtained from the same batch of oocytes. The time of constant recovery from inactivation between batches of oocytes could vary approximately twofold.

structural hypothesis. In addition, part of the acidic domain at the N-terminus seems to contribute to subunit recognition and assembly (Xu et al., 1995). Thus it is difficult to imagine that interactions that depend on the inactivated state of the channel may grossly alter the stability of the channel oligomer.

Relation to other studies

Other studies of voltage-gated K^+ channels have applied deletion analysis to investigate the functional significance of cytoplasmic N- and C-terminal domains. While bearing in mind that the termini of these channels are highly divergent, especially the cytoplasmic C-terminal region, we have attempted to relate our results to those from similar studies. For instance, VanDongen et al. found that deletions of 16 residues at the N-terminus or 318 residues at the C-terminus of rKv2.1 (a delayed rectifier K^+ channel) caused slower inactivation and slightly altered voltage dependence (VanDongen et al., 1990). These findings may have no direct relation to our study because inactivation of rKv2.1 is more than 2 orders of magnitude slower than fast inactivation of mKv4.1. In addition, their study reported that a double deletion that removed 139 residues at the N-terminus and 318 residues at the C-terminus restored the wild-type phenotype. Our double deletion in mKv4.1 (Δ2-71/Δ494-651) did not cause this effect. In fact, the phenotype of this deletion mutant simply resembled that of Δ2-71 or Δ494-651 alone. In another instance, to test whether differences in the time course of inactivation and recovery from inactiva-

tion were related to divergent C-terminal regions in Shaker K^+ channels (Iverson and Rudy, 1990), Hoshi et al. created C-terminal deletions of ShakerA and ShakerB (Hoshi et al., 1991). They found that deletion of the cytoplasmic C-terminal region had little or no effect on N-type or C-type inactivation and demonstrated that kinetic differences between ShakerA and ShakerB were almost fully explained by a single substitution (valine to alanine) within the first half of S6. We found that C-terminal deletions substantially affected inactivation of mKv4.1 (Figs. 4–6). Finally, Hopkins et al. found that a short deletion at the C-terminal region of Kv1.1 (Δ480-495, the last 15 residues of the polypeptide) increased the time constant of slow inactivation (Hopkins et al., 1994). Again, this process is about 2 orders of magnitude slower than rapid inactivation in mKv4.1, and we found that deletion of the last 96 residues at the C-terminus of mKv4.1 caused no effect. Other studies have used deletion analysis to study subunit assembly of K^+ channels (e.g. Shen et al., 1993). These studies have helped to establish that a region at the N-terminus (named tetramerization domain) is critical for subunit assembly and subfamily-specific subunit association (Shen et al., 1993; Xu et al., 1995). Our study does not directly address this issue. However, because various mutations studied here affected functional expression, we have speculated that intersubunit interactions between N- and C-terminal domains may also help to stabilize the channel oligomer.

CONCLUSION AND FINAL REMARKS

Based on the functional analysis of various deletion mutants, we concluded that rapid inactivation of mKv4.1 K^+ channels may involve a concerted action of the cytoplasmic N- and C-terminal domains. The amphipathic N-terminal region of mKv4.1 is likely to be the inactivation gate. However, its ability to cause channel inactivation seems to depend on the presence of a positively charged domain within the C-terminal region. Thus, by contrast to ShakerB K^+ channels (and other Shaker-related channels), the cytoplasmic C-terminal region is also a key determinant of rapid inactivation gating in mKv4.1 K^+ channels and probably other members of the Shal family (because the regions studied here are highly conserved in other members of this family). Consistent with the idea of an apparently distinct mechanism of inactivation gating, additional electrophysiological and structural analyses indicated that N-type and C-type inactivation are not present in mKv4.1.

This work constitutes part of HJ's Ph.D. thesis proposal. We are grateful to Drs. Richard Horn and Michael O'Leary for critical reading of this manuscript. We also thank Mr. Edward Beck for harvesting *Xenopus* oocytes and performing macropatch experiments shown in Fig. 8 A.

This work was supported by a research grant from the National Institutes of Health (NS32337) to MC. HJ was supported by a departmental training grant from the National Institutes of Health (AA07463).

REFERENCES

Baldwin, T. J., M. Tsaur, G. A. Lopez, Y. N. Jan, and L. Y. Jan. 1991. Characterization of a mammalian cDNA for an inactivating voltage-sensitive K^+ channel. *Neuron.* 7:471–483.

Baro, D. J., L. M. Coniglio, C. L. Cole, H. E., Rodriguez, J. K. Lubell, M. T. Kim, and R. M. Harris-Warrick. 1996. Lobster Shal: comparison with *Drosophila* Shal and native potassium currents in identified neurons. *J. Neurosci.* 16:1689–1701.

Baukrowitz, T., and G. Yellen. 1995. Modulation of K^+ current by frequency and external $[K^+]$: a tale of two inactivation mechanisms. *Neuron.* 15:951–960.

Chabala, L. D., N. Bakry, and M. Covarrubias. 1993. Low molecular weight poly(A)$^+$ mRNA species encode factors that modulate gating of a non-*Shaker* A-type K^+ channel *J. Gen. Physiol.* 102:713–728.

Choi, K. L., R. W. Aldrich, and G. Yellen. 1991. Tetraethylammonium blockade distinguishes two inactivation mechanisms in voltage-activated K^+ channels. *Proc. Natl. Acad. Sci. USA.* 88:5092–5095.

Covarrubias, M., A. Wei, L. Salkoff, and T. B. Vyas. 1994. Elimination of rapid potassium channel inactivation by phosphorylation of the inactivation gate. *Neuron.* 13:1403–1412.

Demo, S. D., and G. Yellen. 1991. The inactivation gate of the Shaker K^+ channel behaves like an open-chennel blocker. *Neuron.* 7:743–753.

Hille, B. 1992. Ionic Channels of Excitable Membranes, 2nd Ed. Sinauer Associates, Sunderland, MA. 116–121.

Hopkins, W. F., V. Demas, and B. Tempel. 1994. Both N- and C-terminal regions contribute to the assembly and functional expression of homo- and heteromultimeric voltage-gated K^+ channels. *J. Neurosci.* 14: 1385–1393.

Hoshi, T., W. N. Zagotta, and R. W. Aldrich. 1990. Biophysical and molecular mechanisms of Shaker potassium channel inactivation. *Science.* 250:533–568.

Hoshi, T., W. N. Zagotta, and R. W. Aldrich. 1991. Two types of inactivation in Shaker K^+ channels: effects of alterations in the carboxy-terminal region. *Neuron.* 7:547–556.

Iverson, L. E., and B. Rudy. 1990. The role of the divergent amino and carboxyl domains on the inactivation of potassium channels derived from the Shaker gene of *Drosophila. J. Neurosci.* 10:2903–2916.

Kowdley, G. C., S. J. Ackerman, J. E. John, L. R. Jones, and J. R. Moorman. 1994. Hyperpolarization-activated chloride currents in Xenopus oocytes. *J. Gen. Physiol.* 103:217–230.

Liu, Y., M. E. Jurman, and G. Yellen. 1996. Dynamic rearrangement of the outer mouth of a K^+ channel during gating. *Neuron.* 16:859–867.

Lopez-Barneo, J., T. Hoshi, S. H. Heinemann, and R. W. Aldrich. 1993. Effects of external cations and mutations in the pore region on C-type inactivation of Shaker potassium channels. *Recept. Channels.* 1:61–71.

MacKinnon, R., R. W. Aldrich, and A. W. Lee. 1993. Functional stoichiometry of Shaker potassium channel inactivation. *Science.* 262:757–759.

Murrell-Lagnado, R. D., and R. W. Aldrich. 1993a. Interactions of the amino terminal domains of Shaker K^+ channels with a pore blocking site studied with synthetic peptides. *J. Gen. Physiol.* 102:949–975.

Murrell-Lagnado, R. D., and R. W. Aldrich. 1993b. Energetics of Shaker K^+ channels blocked by inactivation peptides. *J. Gen. Physiol.* 102: 977–1003.

Ogielska, E. M., W. N. Zagotta, T. Hoshi, S. H. Heinemann, J. Haab, and R. W. Aldrich. 1995. Cooperative subunit interaction in C-type inactivation of K^+ channels. *Biophys. J.* 69:2449–2457.

O'Leary, M. E., L.-Q. Chen, R. Kallen, and R. Horn. 1995. A molecular link between activation and inactivation of sodium channels. *J. Gen. Physiol.* 106:641–658.

Pak, M. D., K. Baker, M. Covarrubias, A. Butler, A. Ratcliffe, and L. Salkoff. 1991. mShal, a subfamily of A-type K^+ channel cloned from mammalian brain. *Proc. Natl. Acad. Sci. USA.* 88:4386–4390.

Panyi, G., Z. Sheng, L. Tu, and C. Deutsch. 1995. C-type inactivation of a voltage-gated K^+ channel occurs by a coopertive mechanism. *Biophys. J.* 69:896–903.

Ruppersberg, J. P., R. Frank, O. Pongs, and M. Stocker. 1991. Cloned neuronal Ik(A) channels reopen during recovery from inactivation. *Nature.* 353:657–660.

Salkoff, L., K. Baker, A. Butler, M. Covarrubias, M. D. Pak, and A. Wei. 1992. An essential "set" of K^+ channels conserved in flies, mice and humans. *Trends Neurosci.* 15:161–166.

Serodio, P., C. Kentros, and B. Rudy. 1994. Identification of molecular components of A-type channels activating at subthreshold potentials. *J. Neurophys.* 72:1516–1529.

Serodio, P., E. Vega-Saenz de Miera, and B. Rudy. 1996. Cloning of a novel component of A-type K^+ channel operating at subthreshold potentials with unique expression in heart and brain. *J. Neurophysiol.* 75:2174–2179.

Shen, N. V., X. Chen, M. M. Boyer, and P. J. Pfaffinger. 1993. Deletion analysis of K^+ channel assembly. *Neuron.* 11:67–76.

Sheng, M., M.-L. Tsaur, Y. N. Jan, and L. Y. Jan. 1992. Subcellular segregation of two A-type K^+ channel proteins in rat central neurons. *Neuron.* 9:271–284.

Spector, P. S., M. E. Curran, A. Zou, M. Keating, and M. C. Sanguinetti. 1996. Fast inactivation causes rectification of the I_{Kr} channel. *J. Gen. Physiol.* 107:611–619.

Tseng-Crank, J.-A., J. Yao, M. F. Berman, and G.-N. Tseng. 1993. Functional role of the NH2-terminal cytoplasmic domain of a mammalian A-type K^+ channel. *J. Gen. Physiol.* 102:1057–1083.

VanDongen, A. M. J., G. C. Frech, J. A. Drewe, R. H. Joho, and A. M. Brown. 1990. Alteration and restoration of K^+ channel function by deletions at the N- and C-termini. *Neuron.* 5:433–443.

West, J. W., D. E. Patton, T. Scheuer, Y. Wang, A. L. Goldin, and W. A. Catterall. 1992. A cluster of hydrophobic amino acid residues required for fast Na^+-channel inactivation. *Proc. Natl. Acad. Sci. USA.* 89: 10910–10914.

Xu, J., W. Yu, Y. N. Jan, L. Y. Jan, and M. Li. 1995. Assembly of voltage-gated potassium channels: conserved hydrophilic motifs determine subfamily-specific interactions between the alpha-subunits. *J. Biol. Chem.* 270:24761–24768.

Zagotta, W. N., T. Hoshi, and R. W. Aldrich. 1990. Restoration of inactivation in mutants of Shaker potassium channel by a peptide derived from ShB. *Science.* 250:568–571.Equation 1